Selective Inhibition of the C-Domain of Angiotensin I Converting Enzyme by Bradykinin Potentiating Peptides

Joël Cotton,[‡] Mirian A. F. Hayashi,[§] Philippe Cuniasse,[‡] Gilles Vazeux,[‡] Danielle Ianzer,[§] Antonio C. M. De Camargo,[§] and Vincent Dive*[,‡]

CEA, Département d'Ingénierie et d'Etudes des Protéines (DIEP), CE-Saclay, 91191 Gif/Yvette Cedex, France, and Instituto Butantan, Depto. Bioquimica e Biofisica, Av. Vital Brasil, 1500 Sao Paulo-SP, Brazil

Received December 5, 2001; Revised Manuscript Received February 11, 2002

ABSTRACT: Somatic angiotensin I converting enzyme (ACE) contains two functional active sites. Up to now, most of the studies aimed at characterizing the selectivity of inhibitors toward the two ACE active sites relied on the use of ACE mutants containing a single functional active site. By developing new fluorogenic synthetic substrates of ACE, we demonstrated that inhibitor selectivity can be assessed directly by using somatic ACE. This useful screening approach led us to discover that some bradykinin potentiating peptides turned out to be selective inhibitors of the C-domain of ACE. The peptide pGlu-Gly-Leu-Pro-Pro-Arg-Pro-Lys-Ile-Pro-Pro, with K_i(app) values of 30 nM and 8 μM, respectively, for the C- and N-domain of ACE, is to our knowledge the most highly selective C-domain inhibitor of ACE so far reported. Inhibitors able to block selectively either the N- or C-domain of ACE will represent unique tools to probe the function of each domain in the regulation of blood pressure or other physiopathological events involving ACE activity.

Angiotensin converting enzyme (ACE)[1] (peptidyl dipeptidase A, EC 3.4.15.1) is a key player in the regulation of blood pressure and cardiovascular function. ACE inhibitors are widely used for the treatment of patients with high blood pressure, cardiac failure, and diabetic nephropathy (*1*). The antihypertensive effect of ACE inhibitors is explained not only by prevention of the formation of angiotensin II (Ang II) but also by potentiation of the hypotensive effects of bradykinin (BK) (*2*).

Bradykinin potentiating peptides (BPPs) present in snake venom were the first naturally occurring ACE inhibitors described (*3*−*9*). BPPs were also the first compounds able to block potently in vivo ACE activity and prevent the blood pressure increases induced by Ang I injection, by blocking the conversion of Ang I into Ang II (*10*−*12*). Structure−activity studies of BPPs were essential for the development of the ACE inhibitors currently used clinically as antihypertensive agents (*13*).

Following these pioneering studies, the primary structure of human endothelial somatic ACE was determined, revealing the unexpected presence of two homologous domains (*14*). Each domain contains an active site, characterized by the presence of a zinc metallopeptidase consensus sequence and whose functionality was demonstrated by site-directed mutagenesis (*15*). The discovery that somatic ACE contains two active sites has stimulated many attempts to establish whether they may differ, leading each domain to control distinct physiological functions. Such investigations were mainly hampered by the lack of inhibitors able to differentiate markedly the two ACE active sites (*16*−*19*). By screening phosphinic peptide libraries, RXP407 was recently identified as the first N-selective inhibitor of ACE, able to differentiate the two ACE active sites with a selectivity factor of roughly 3 orders of magnitude (*20*). RXP407 was shown, in vivo, to block selectively the cleavage of the Ac-S-D-K-P peptide (*21*), a substrate mostly cleaved in vitro (*22*) and in vivo (*23*) by the ACE N-domain. In contrast, blood pressure response to exogenous angiotensin I was not affected by RXP407 (*21*). These results suggest that the cleavage of angiotensin I in vivo could be controlled solely by the C-domain of ACE. To check this hypothesis, a search for highly selective inhibitors of the C-domain was undertaken.

The development of dual fluorogenic substrates of ACE, endowed with defined specificity for each of the two ACE active sites, was a crucial step for the development of a screening project. In this paper, the properties of such fluorogenic ACE substrates are described, and their value in easy identification of selective inhibitors of ACE is demonstrated. Among the compounds that were screened, we discovered that some BPPs displayed selectivity toward the C-domain of ACE. The potency and selectivity toward ACE of the BPPs that were the most studied previously (BPPa, BPPb, BPPc, and BPP2, Scheme 1) were determined. The potential value of selective inhibitors of ACE is discussed in light of new results regarding the possible function of the two ACE active sites and the effects of ACE inhibitors on the potentiation of BK.

* Address correspondence to this author. Tel: (33) 1 69083585. Fax: (33) 1 69089071. E-mail: vincent.dive@cea.fr.

[‡] CEA, Département d'Ingénierie et d'Etudes des Protéines.

[§] Instituto Butantan, Depto. Bioquimica e Biofisica.

[1] Abbreviations: ACE, angiotensin converting enzyme; Mca, 7-methoxycoumarin-2-acetic acid; DpaOH, *N*3-(2,4-dinitrophenyl)-L-2,3-diaminopropionyl; McaAla, Mca-Ala-Ser-Asp-Lys-DpaOH; McaSer, Mca-Ser-Asp-Lys-DpaOH.

10.1021/bi012121x CCC: $22.00
Published on Web 04/20/2002

Scheme 1

pGlu^{9}-**Trp^{8}**-Pro^{7}-Arg^{6}-Pro^{5}-**Gln^{4}**-Ile^{3}-Pro^{2}-Pro^{1} BPPa

pGlu^{11}-Gly^{10}-Leu^{9}-Pro^{8}-Pro^{7}-Arg^{6}-Pro^{5}-**Lys^{4}**-Ile^{3}-Pro^{2}-Pro^{1} BPPb

pGlu^{11}-Gly^{10}-Leu^{9}-Pro^{8}-Pro^{7}-**Gly^{6}**-Pro^{5}-**Pro^{4}**-Ile^{3}-Pro^{2}-Pro^{1} BPPc

pGlu^{10}-**Asn^{9}**-**Trp^{8}**-Pro^{7}-**His^{6}**-Pro^{5}-**Gln^{4}**-Ile^{3}-Pro^{2}-Pro^{1} BPP2

EXPERIMENTAL PROCEDURES

Materials. Human wild-type somatic ACE and ACE mutants, containing only one functional active site, were obtained through stable expression in Chinese hamster ovary cells transfected with appropriate ACE cDNA (*15*). This material was kindly provided by Professor P. Corvol of the Institut National de la Santé et de la Recherche Médicale, Unité 36. Expression and purification of ACE were performed as previously described (*15*). Mca-Ser-Asp-Lys-DpaOH (McaSer) substrate was prepared following the procedure described for Mca-Ala-Ser-Asp-Lys-DpaOH (McaAla) (*20*). BPPa, BPPb, and BBPc peptides were from Bachem. BPP2 was synthesized by solid-phase synthesis, using the sequence previously reported *(24)*.

Enzyme Assays. Assays were carried out at 25 °C in 50 mM Hepes, pH 6.8, 200 mM NaCl, and 10 μM $ZnCl_2$. Continuous assays were performed by recording the fluorescence increase at 390 nm ($\lambda_{ex} = 340$ nm) induced by the cleavage of McaAla and McaSer substrates by ACE, using black, flat-bottomed, 96-well nonbinding surface plates (Corning Costar France). Fluorescence signals were monitored using a Biolumin 960 photon counter spectrophotometer (Molecular Dynamics) equipped with a temperature control device and a plate shaker. The substrate and enzyme concentrations for the experiments were chosen so as to remain well below 10% of substrate utilization and observe initial rates. Concentrations of substrate solutions, prepared in dimethyl sulfoxide, were determined spectrophotometrically using $\epsilon_{328nm} = 12900\ M^{-1}\ cm^{-1}$. The kinetic parameters K_m and k_{cat} for the hydrolysis of the substrates McaAla and McaSer by the ACE mutants were determined using the direct linear plot method (*25*−*27*). This method allows determination of confidence intervals on k_{cat} and k_{cat}/K_m (*28*). The same approach was also used to determine apparent k_{cat}/K_m for the cleavage of McaAla and McaSer by somatic ACE. These kinetic parameters were determined using a substrate concentration range of 5−80 μM. A correction factor for each substrate concentration, determined experimentally, was used to correct for the inner filter effect, as described before (*29*).

Inhibition Studies. Inhibitors were dissolved in buffer containing either the McaAla or McaSer substrate ($S = K_m$). The reaction was initiated by addition of ACE. Enzyme concentrations were chosen in order to observe steady-state rates of hydrolysis over a period of 40 min. Data were collected for 25 min, every 10 s. For BPP peptides, no sign of slow binding was evident from the progress curves. Experimental conditions to study lisinopril were previously described (*30*). In the presence of RXP407, there is a time-dependent decrease in the steady-state rate, which is a function of the inhibitor concentration, suggesting the occurrence of a slow-binding inhibition mechanism. Preincubation experiments indicated that, given the RXP407 concentration range, stable ACE inhibition requires incubation of the enzyme and RXP407 for at least 45 min. Such a long time precludes the observation of the equilibrium before depletion of the substrate. Thus, inhibition studies with RXP407 were performed by equilibrating increasing concentrations of RXP407 with ACE (45 min) and then initiating the reaction by adding the substrate to determine the residual free enzyme concentration. Due to the slow dissociation of RXP407 from ACE, it was possible to neglect the effect of substrate addition on the equilibrium position and to observe stable steady-state rate on the time scale of monitoring.

Inhibitor concentrations were selected in order to observe a full range of inhibition percentages.

When the inhibition experiments were performed with the ACE mutants, K_i values were determined using the method of Horovitz and Levitzki (*31*). All K_i values reported were reproducible within ±5%. When wild-type somatic ACE was used, K_i(app) values were estimated from simulation, as described below.

Simulations. Theoretical inhibition profiles of somatic ACE with the different inhibitors were simulated by using the program DYNAFIT from P. Kuzmic (*32*). This program describes the system under consideration by a set of kinetic equations that correspond to substrate cleavage and inhibitor binding. ACE was modeled as two independent sites, each site being able to cleave the substrate with specific kinetic parameters. Comparison of the K_m and k_{cat} values obtained for the cleavage of McaAla and McaSer substrates using ACE mutants with the values determined with somatic ACE (data not shown) was consistent with this hypothesis. The six equilibria used to model ACE are shown in Scheme 2. In this scheme, E1 and E2 refer respectively to the N- and C-domains of ACE.

Scheme 2

$$E1 + S \underset{k_{off1}}{\overset{k_{on}}{\rightleftharpoons}} E1S \quad (1)$$

$$E2 + S \underset{k_{off2}}{\overset{k_{on}}{\rightleftharpoons}} E2S \quad (2)$$

$$E1S \xrightarrow{k_{cat1}} E1 + P \quad (3)$$

$$E2S \xrightarrow{k_{cat2}} E2 + P \quad (4)$$

$$E1 + I \underset{k_{offi1}}{\overset{k_{on}}{\rightleftharpoons}} E1I \quad (5)$$

$$E2 + I \underset{k_{offi2}}{\overset{k_{on}}{\rightleftharpoons}} E2I \quad (6)$$

Simulations using Dynafit require to explicitly set all kinetic constants. With the exception of RXP407, k_{on} values were set to $10^8\ M^{-1}\ s^{-1}$ for all equilibria. k_{off} values for the substrate hydrolysis (k_{off1} and k_{off2}, equilibria 1 and 2 in Scheme 2) were set according to the Michaelis model $k_{off1,2} = (k_{on}K_{m1,2}) - k_{cat1,2}$. For inhibitors, kinetic constants ($k_{off3,4}$) were calculated according to $k_{off3,4} = k_{on}K_{i1,2}$. In the specific case of the RXP407 interaction with the N-domain of ACE, the k_{on} value was determined experimentally. Twelve progress curves, observed just after the addition of somatic ACE on solutions containing the substrate and the inhibitors, at

Table 1: Kinetic Parameters for the Hydrolysis of the McaAla and McaSer Substrates by the ACE Mutants, Obtained by Using the Direct Plot Method[a]

	McaAla	McaSer
K_{m1} (μM)[b]	41 (38−46)	39 (37−42)
K_{m2} (μM)[b]	46 (45−48)	36 (35−38)
k_{cat1} (s^{-1})	15.9	3.5
k_{cat2} (s^{-1})	15.9	12.9
k_{cat1}/K_{m1} ($s^{-1}\cdot\mu M^{-1}$)[b]	0.38 (0.34−0.42)	0.089 (0.07−0.1)
k_{cat2}/K_{m2} ($s^{-1}\cdot\mu M^{-1}$)[b]	0.34 (0.32−0.36)	0.36 (0.33−0.39)
k_{off1} (s^{-1})[c]	4074	3896
k_{off2} (s^{-1})[c]	4624	3587

[a] 1 refers to the ACE mutant containing only the functional N-terminal active site and 2 to a functional C-terminal active site. Conditions: 50 mM Hepes, pH 6.8, 200 mM NaCl, and 10 μM $ZnCl_2$. [b] The confidence limits on the k_{cat} and k_{cat}/K_m values are indicated in parentheses. [c] Calculated values, as described in Experimental Procedures.

different inhibitor concentrations, were recorded. A global least-squares fit of these progress curves provided k_{on} and k_{off} (*32*). The k_{on} value determined for the interaction of RXP407 with the N-domain of somatic ACE was 2.4×10^4 M^{-1} s^{-1}.

The K_i(app) values reported in Table 2 were obtained as follows: Initial values of K_{i1} and K_{i2} were set to simulate progress curves, using experimental inhibitor concentrations. A similar progress curve was calculated in the absence of inhibitor. Steady-state velocities were determined from these curves. For each inhibitor concentration, the percentage of inhibition was calculated as the ratio of the steady-state velocity in the absence and presence of inhibitor. The initial values of K_{i1} and K_{i2} were varied until a good agreement between the simulated and the experimental inhibition curves was obtained. The K_i(app) values reported in Table 2 corresponded to the most satisfactory simulation (displayed in Figure 3a,c). This procedure makes difficult the estimation of the uncertainty on K_{i1} and K_{i2}, as these values were not obtained from a regression analysis. The uncertainty on the K_i(app) values was estimated as described below. For a set of estimated K_{i1}, K_{i2}, the uncertainty on K_{i1} was determined by simulating a curve that crosses the point showing the largest deviation from the model, in the region corresponding to the titration of site 1. A similar calculation was carried out to determine the uncertainty on K_{i2}. In all cases, the uncertainty on K_i(app) reported in Table 2 was lower than 50%.

RESULTS

Theoretical Model of ACE Inhibition. The kinetic parameters K_m and k_{cat} for the degradation of the new fluorogenic substrate Mca-Ser-Asp-Lys-DpaOH (McaSer) by the N- and C-domain ACE mutants indicated that this substrate is more efficiently cleaved by the C-domain than by the N-domain of ACE (k_{cat}/K_m of 0.36 $s^{-1}\cdot\mu M^{-1}$ for the C-domain and 0.089 $s^{-1}\cdot\mu M^{-1}$ for the N-domain; Table 1). This selectivity is mostly due to a higher k_{cat} value displayed by this substrate toward the C-domain, as compared to the N-domain (12.9 versus 3.5 s^{-1}). Interestingly, this new fluorogenic substrate, when used in combination with the previously reported fluorogenic substrate Mca-Ala-Ser-Asp-Lys-DpaOH (McaAla) (*20*), turned out to be a convenient tool for screening tests aimed at identifying inhibitors able to block selectively either the N- or the C-domain active site of somatic ACE. To exemplify this property, a number of simulations were performed to determine the inhibition profiles that should be observed with these substrates when somatic ACE is inhibited by compounds able to differentiate the two active sites of this enzyme. These simulations were performed by considering the case where the inhibitor displayed a K_i value of either 1 or 10 nM for one site and a K_i value of 1 μM for the other one (selectivity of 3 or 2 orders of magnitude, respectively). As shown in Figure 1a,b, the titration profiles using the McaSer substrate are extremely dependent on the inhibitor specificity. Such profiles can thus be used to identify either a C- or an N-selective inhibitor, with a selectivity factor of 1000 and 100, respectively. Similar simulations, but performed with the McaAla substrate (Figure 1c,d), revealed that the inhibition profiles differ much less than those generated with McaSer. Thus, depending of the experimental uncertainties, it might be more difficult to determine with confidence whether an inhibitor, displaying a selectivity lower than 2 orders of magnitude, is N- or C-selective using the McaAla substrate alone. These simulations led us to consider that it would be convenient for screening tests to determine systematically the percentage inhibition for any compound using both McaAla and McaSer substrates. Inspection of Figure 2a,b demonstrates that a C-selective inhibitor is manifested when the percentage of inhibition observed with the McaSer is higher than that obtained with McaAla. The reverse situation is typical of an N-selective inhibitor (Figure 2c,d). In the case of an inhibitor displaying a selectivity factor of 100 (Figure 2b,d), the simulations indicate that the inhibition profiles obtained with the two substrates should exhibit, at some inhibitor concentrations, differences in the percentage of inhibition of 30%. Thus, this approach based on dual fluorogenic substrates should allow to identify with good confidence inhibitors displaying selectivity of at least 2 orders of magnitude.

Validation of the Approach with RXP407, an N-Selective Inhibitor of ACE. The phosphinic peptide RXP407 is the first potent inhibitor of ACE that was reported to be able to differentiate the two ACE active sites, with a selectivity factor of about 3 orders of magnitude (*20*). The experimental titration curves obtained for the inhibition of wild-type ACE by RXP407 with McaAla and McaSer are reported in Figure 3a (closed circles). The higher percentage of inhibition, when the substrate used is McaAla, is consistent with the fact that RXP07 is an N-selective inhibitor of ACE (compared with Figure 2c,d). As shown in Figure 3a, inhibition curves can be simulated (continuous lines) that reproduced fairly well the experimental data obtained with the two substrates. From these two simulations, the same K_i(app) value (7 nM) was estimated for the interaction of RXP407 with the N-domain of ACE. However, the K_i(app) values determined for the interaction of RXP407 with the C-domain were slightly different, 4 and 1 μM (Table 2). From direct binding experiments with tritiated RXP407, a K_D value of 9 nM was determined for the interaction of this inhibitor with the N-domain of wild-type ACE (*30*). A K_i value of 2−3 μM was obtained for the interaction of RXP407 with the geminal form of ACE, a form containing only the C-domain of ACE (*30*). Thus, overall the comparison of the K_D or K_i values previously reported with the K_i(app) given in Table 2 led us to suggest not only that McaAla and McaSer substrates can be used to identify easily selective inhibitors of ACE but

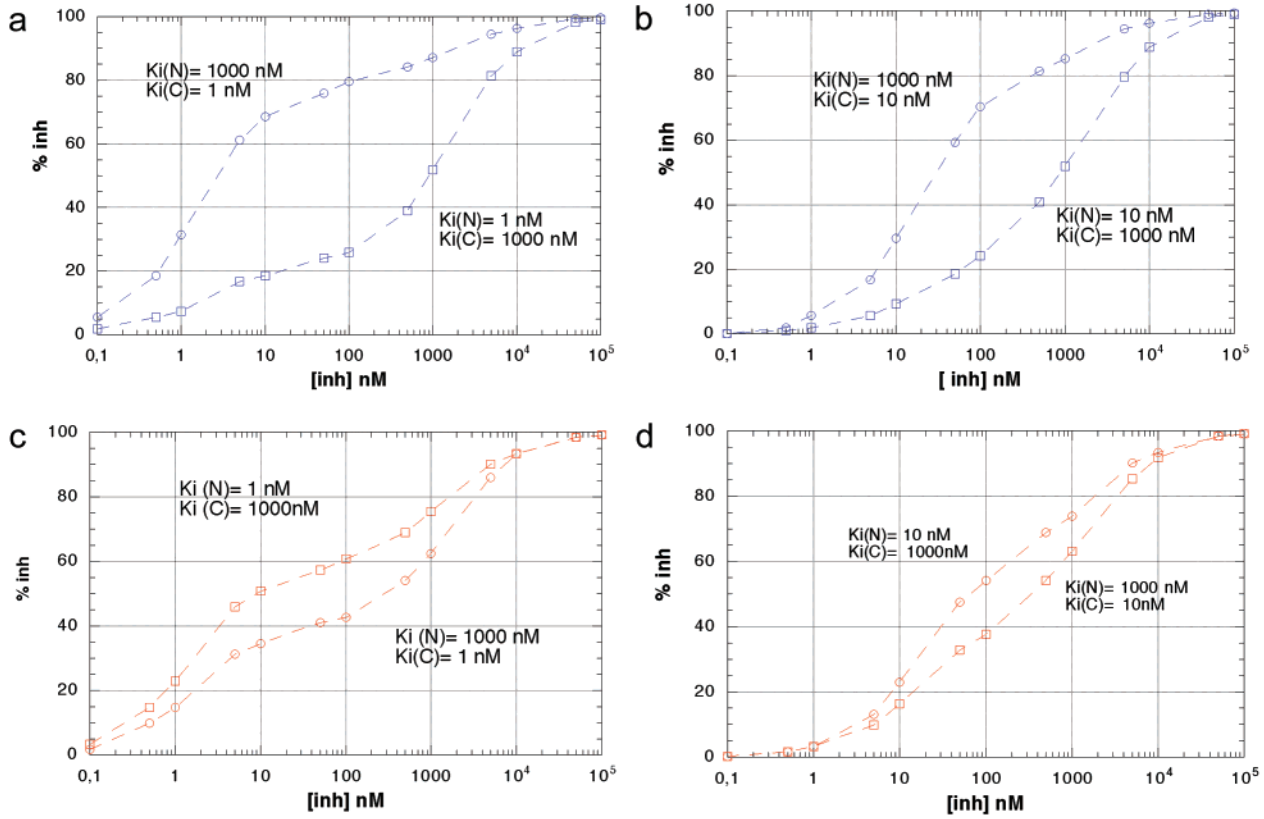

FIGURE 1: Simulated profiles for the inhibition of somatic ACE by either C- or N-selective inhibitors possessing a selectivity factor of 1000 and 100. The inhibition profiles are those expected when using the McaSer (a, b) and McaAla (c, d) substrates.

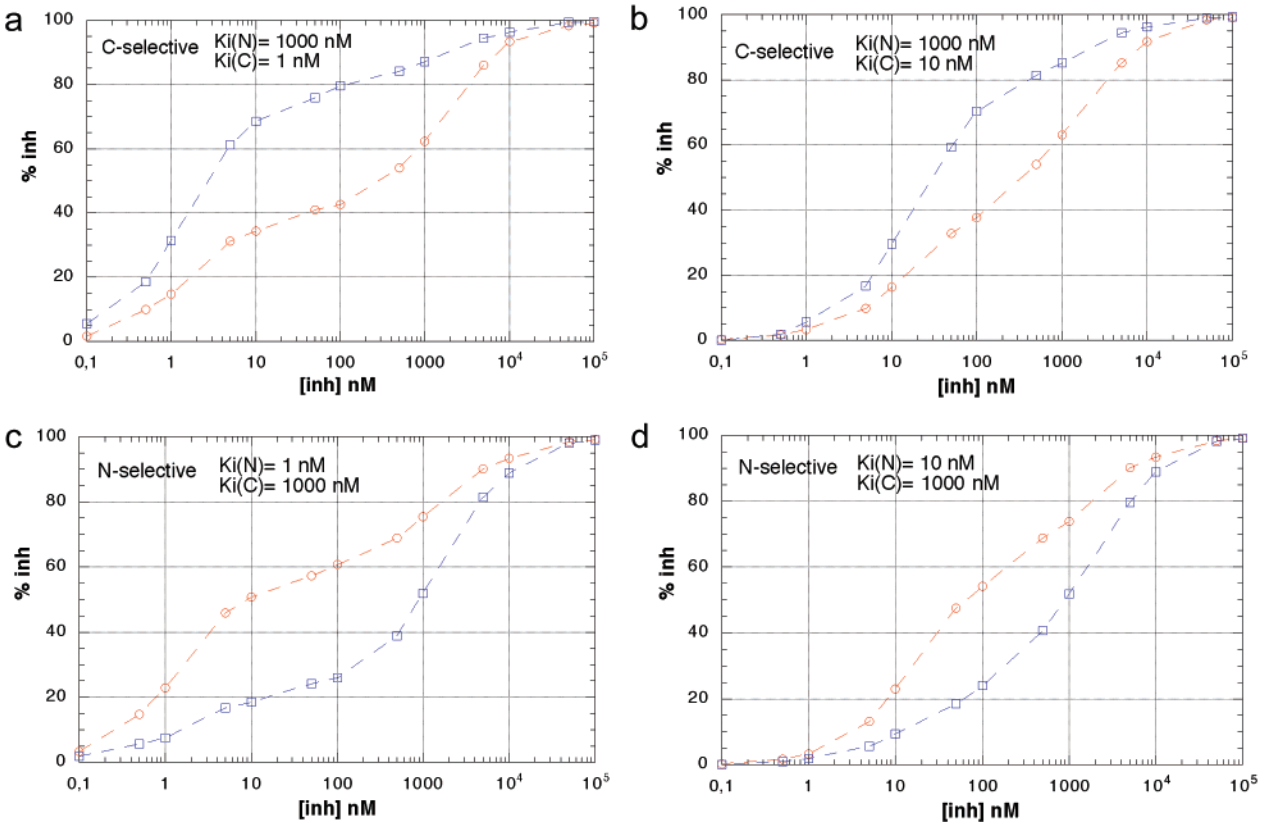

FIGURE 2: Simulated inhibition profiles of somatic ACE. Panels a and b display profiles when the substrate is either McaSer (blue curve) or McaAla (red curve) and when a C-selective inhibitor possesses a selectivity factor of 1000 (a) or 100 (b). Panels c and d display profiles when the substrate is either McaSer (blue curve) or McaAla (red curve) and when an N-selective inhibitor possesses a selectivity factor of 1000 (c) or 100 (d).

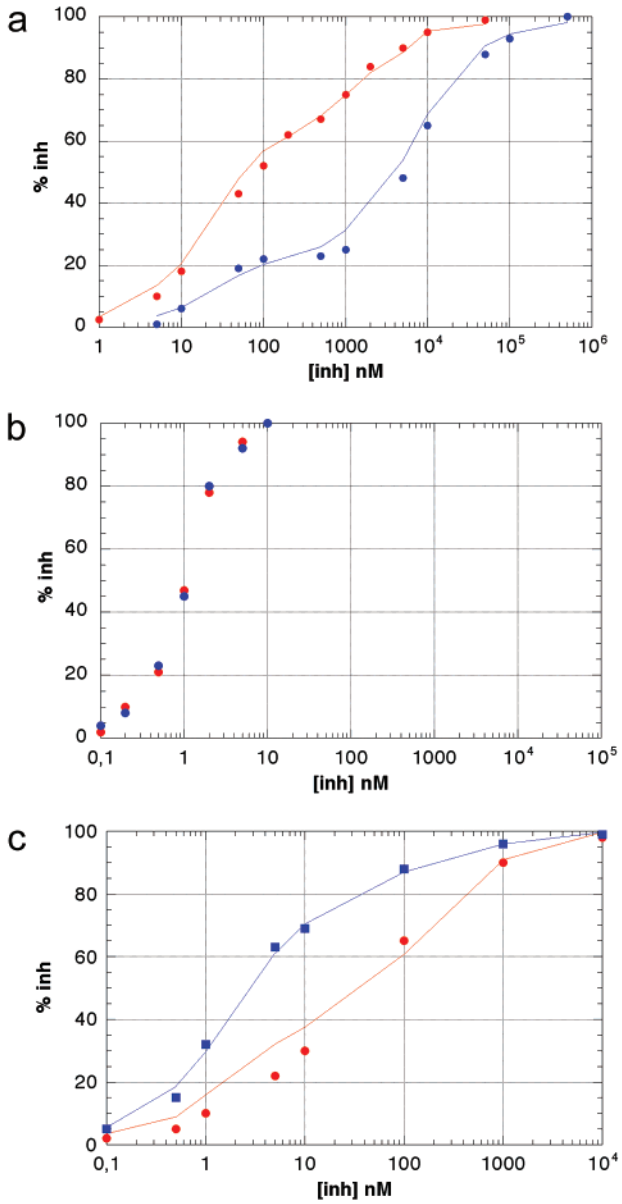

FIGURE 3: (a) Inhibition profiles of somatic ACE by RXP407 when the substrate used is McaAla (red curve) or McaSer (blue curve). Closed circles correspond to experimental data. Continuous lines display simulated profiles obtained with K_i values of 7 nM and 1−4 μM, corresponding respectively to the interaction of RXP407 with the N- and C-domains of somatic ACE. (b) Profiles for the inhibition of somatic ACE by lisinopril when the substrate is McaAla (red points) or McaSer (blue points). (c) Profiles for the inhibition of somatic ACE by BPPa when the substrate used is McaAla (red curve) or McaSer (blue curve). Closed circles correspond to experimental data. Continuous lines display simulated profiles obtained with K_i values of 1 and 100 nM, corresponding respectively to the interaction of BPPa with the C- and N-domains of somatic ACE.

also that reasonable estimates of their affinities can be determined, as far as a good agreement was observed between experimental data and simulations.

Inhibition Profiles with Lisinopril. With lisinopril, the two inhibition profiles observed with the McaAla and McaSer substrates were superimposed (Figure 3b). This superimposition is in agreement with the results previously reported by Michaud et al., showing that lisinopril inhibited the N- and C-domain ACE mutant with a similar potency (*19*). The very different inhibition profiles observed between lisinopril and RXP407 exemplify how the use of these dual fluorogenic substrates can easily identify mixed or selective ACE inhibitors.

Table 2: Potency and Selectivity of BPPs toward the N- and C-Domains of Somatic ACE[a]

	K_i(app) values (nM)			
	McaAla substrate		McaSer substrate	
	N-domain	C-domain	N-domain	C-domain
RXP407	7	1000	7	4000
BBPa	100	1	100 (80)	1 (0.5)
BPPb	10000	30	8000 (9000)	30 (25)
BPPc	80	80	80 (55)	80 (70)
BPP2	200	1.5	200 (220)	1.5 (2)

[a] K_i(app) values were determined from the simulations that best reproduced the experimental data. Values in parentheses were determined with ACE mutants, containing a single functional active site, using McaSer as substrate.

Potency and Selectivity of Bradykinin-Potentiating Peptides. From the experimental inhibition profiles obtained with BPPa (Figure 3c, closed circles), it can be seen that the percentage inhibition at low BBPa concentrations (1−50 nM) is higher with McaSer than McaAla (70% versus 30%, respectively, at 10 nM BPPa). On the basis of the above considerations, these results revealed that BPPa preferentially interacts with the C-domain of ACE. Experimental data were rather well reproduced by the simulated curves (Figure 3c, continuous lines). From these simulations, K_i(app) values of 1 and 100 nM were estimated for the interactions of BPPa with the C- and N-domains of ACE, respectively (Table 2). The K_i(app) values estimated for the other BPPs, using the same approach, revealed that BPPb and BPP2 also behaved as C-selective inhibitors of ACE, BPPb exhibiting the highest selectivity. BPPc turned out to be a mixed ACE inhibitor. Comparison of the K_i(app) values estimated with the approach outlined above with the K_i values determined using ACE mutants, containing a single functional active site (Table 2, values into parentheses), confirms that our approach provides indeed a fairly good estimate of the actual inhibitor potency.

DISCUSSION

Despite the huge numbers of biochemical studies of ACE performed over the last 3 decades, very few convenient synthetic fluorogenic substrates have been developed for this enzyme (*20*, *33*, *34*). Due to the key role of ACE in human health, most of the research was directed toward the study of the physiological substrates of ACE, namely, Ang I and BK. We previously reported the use of McaAla as a convenient fluorogenic substrate for routine ACE assays (*20*). On the basis of simulations, we also suggested that dual fluorogenic substrates endowed with a slight difference in selectivity for the N- and C-domain of ACE, like the McaALa and McaSer substrates reported in this study, would represent valuable tools to study the interaction of selective inhibitors with wild-type somatic ACE. Mutants of somatic ACE containing a single functional active site were developed and used in studies aimed at identifying selective inhibitors. While these mutants simplify the interpretation of the inhibition studies, there are many circumstances where the use of somatic ACE may be more appropriate, such as

working with somatic ACE from different sources. Also, as the occurrence of some cooperativity between the two ACE active sites has been discussed in previous studies, investigations of such a cooperative mechanism obviously require to work with somatic ACE (*35*). As shown by the present study, identification of selective inhibitors of somatic ACE is efficiently achieved using dual fluorogenic substrates (McaAla and McaSer), with no requirement of ACE mutants. Due to its simplicity, such an approach constitutes a valuable screening test to identify selective inhibitors of ACE from a large array of compounds. However, several aspects of our approach should be taken into consideration. First, kinetic parameters were determined to describe the cleavage of McaAla and McaSer by the ACE mutants and somatic ACE. By comparing the values of these parameters, we concluded that the mutant parameters can be used to describe the cleavage of these two substrates by somatic ACE activity. In this specific case, somatic ACE can be modeled as two independent active sites. This step was essential in order to simulate inhibition curves and, as shown in Figures 1 and 2, exemplify the influence of the substrate selectivity on these profiles. The second step of our approach concerns the experimental determination of the inhibition profiles, using the McaAla and McaSer substrates. Inhibition curves that do not superimpose reveal the occurrence of selective inhibition of each somatic ACE active site. Finally, simulations were performed in order to determine whether the experimental observations could be reproduced theoretically, using the set of equations reported in Scheme 2. The observation of a reasonable agreement between experimental and simulated inhibition profiles, as observed in this study, affords the conclusion that there is no cooperative process during the binding of the inhibitor to the two active sites of somatic ACE; thus K_i values can be estimated. Under this condition, the estimated K_i values from the simulations are in reasonable agreement with the values deduced from experiments based on the ACE mutants (Table 2). In contrast, if experimental inhibition profiles could not be reproduced by simulations, this may indicate the occurrence of a more complex process, such as a cooperative mechanism for the interaction of the inhibitor with the two ACE active sites.

This study demonstrates for the first time that some BPPs are highly selective inhibitors of the C-domain of ACE. Among the four BPPs examined in this study, BPPb turned out to be the most selective inhibitor of the C-domain reported so far. As compared with the three other BPPs, the higher selectivity of BPPb is explained by a very low affinity for the N-domain of ACE. BPPb displays a K_i(app) value of 8−10 μM for the N-domain, whereas K_i(app) values varying from 80 to 200 nM were determined for the interaction of BPP1, BPP2, and BPPa with the N-domain. The presence of a lysine residue in position 4 of BPPb, instead of glutamine or proline at the same position in other BPPs, may account for the lower affinity of BPPb for the N-domain of ACE. In the same way, the mixed inhibition displayed by BPPc could be ascribed to the presence of proline in position 4 in this compound. BPPa and BPP2 peptides, as compared to BPPb and BPPc, are highly potent inhibitors of the C-domain. The presence of a glutamine (position 4) in the sequence of these two peptides may explain their high potency toward the C-domain. These above remarks about the putative role of position 4 suggest that subtle changes in the sequence of BPPs may affect their potency and selectivity toward the N- or C-domain of ACE. If the nature of the residue in position 4 of these peptides, in addition to their signature sequence Ile-Pro-Pro, seems to play important role in their potency and selectivity, the contribution of the other residues cannot be ruled out. Thus, extensive structure−activity studies would be required before drawing definitive conclusions about the role of each residue. Indeed, preliminary study of several BPP analogues did not provide clear relationships between the structure of these peptides and their ability to differentiate the two ACE active sites (unpublished results).

The availability of highly potent and N- or C-selective inhibitors of ACE, such as RXP407 or BPPb, may contribute to the efforts aimed at discovering whether the ACE gene duplication is associated with particular functions for each domain of this enzyme in mammalian species (*14*). As shown by this study, RXP407 or BPPb modulates significantly the degradation of McaAla and McaSer, despite the weak difference in the relative specificity of the N- and C-domain of ACE in cleaving these two substrates. Thus, depending of the relative specificity of the N- and C-domain of ACE in cleaving physiological substrates, RXP407 and BPPb could potentially in vivo control their metabolism in a selective manner. In vitro, the two ACE domains were proposed to hydrolyze with the same efficiency Ang I and BK (*15*, *17*). However, ACE substrate selectivity is regulated by chloride in a complex manner, the C-domain being the most sensitive to chloride concentration (*15*, *17*). From these considerations, it seems imperative to check whether in vivo a selective control of the Ang I or BK metabolism can be achieved by a selective C-domain inhibitor such as BPPb.

BPPs, as well as synthetic ACE inhibitors, potentiate the effects of BK. Among different mechanisms explaining this property, the inhibition of ACE, the most active player in the inactivation of BK, has been considered (*2*). Our results on the BPPb selectivity suggest that the inactivation of BK could be achieved by blocking only one ACE active site. Marcic et al. recently discussed new mechanisms to account for the potentiation of the BK effects by ACE inhibitors (*36*−*38*). These authors invoked a cross talk between ACE and the BK B_2 receptor, induced by the binding of the inhibitor to ACE. In this respect, it would be also of great interest to study how the BK interaction with its B_2 receptor is influenced after binding of either RXP407 or BPPb to ACE.

Additional structure−function studies will be necessary to decipher the structural elements in the BPP peptides that are critical for their selective interaction with the C-domain of ACE. In the meanwhile, the structure of BPPb may provide a starting point for developing nonpeptidic compounds endowed with high potency and selectivity for the C-domain of ACE that may lead to a new generation of ACE inhibitors.

REFERENCES

1. Waeber, B., Nussberger, J., and Brunner, H. (1995).
2. Linz, W., Wiemer, G., Gohlke, P., Unger, T., and Scholkens, B. A. (1995) *Pharmacol. Rev. 47*, 25−49.
3. Ferreira, S. H., and Rocha e Silva, M. (1965) *Experientia 21*, 347−349.
4. Ferreira, S. H., and Vane, J. R. (1967) *Br. J. Pharmacol. 30*, 417−424.

5. Amorim, D. S., Ferreira, S. H., Manco, J. C., Tanaka, A., Sader, A. A., and Cardoso, S. (1967) *Cardiology 50*, 23−32.
6. Ferreira, S. H., Bartelt, D. C., and Greene, L. J. (1970) *Biochemistry 9*, 2583−2593.
7. Ondetti, M. A., Williams, N. J., Sabo, E. F., Pluscec, J., Weaver, E. R., and Kocy, O. (1971) *Biochemistry 10*, 4033−4039.
8. Kato, H., and Suzuki, T. (1971) *Biochemistry 10*, 972−980.
9. Cheung, H. S., and Cushman, D. W. (1973) *Biochim. Biophys. Acta 293*, 451−463.
10. Miller, E. D., Jr., Samuels, A. I., Haber, E., and Barger, A. C. (1972) *Science 177*, 1108−1109.
11. Gavras, H., Brunner, H. R., Laragh, J. H., Sealey, J. E., Gavras, I., and Vukovich, R. A. (1974) *N. Engl. J. Med. 291*, 817−821.
12. Case, D. B., Wallace, J. M., Keim, H. J., Weber, M. A., Sealey, J. E., and Laragh, J. H. (1977) *N. Engl. J. Med. 296*, 641−646.
13. Ondetti, M. A. (1994) *Annu. Rev. Pharmacol. Toxicol. 34*, 1−16.
14. Soubrier, F., Alhenc-Gelas, F., Hubert, C., Allegrini, J., John, M., Tregear, G., and Corvol, P. (1988) *Proc. Natl. Acad. Sci. U.S.A. 85*, 9386−9390.
15. Wei, L., Alhenc-Gelas, F., Corvol, P., and Clauser, E. (1991) *J. Biol. Chem. 266*, 9002−9008.
16. Wei, L., Clauser, E., Alhenc-Gelas, F., and Corvol, P. (1992) *J. Biol. Chem. 267*, 13398−13405.
17. Jaspard, E., Wei, L., and Alhenc-Gelas, F. (1993) *J. Biol. Chem. 268*, 9496−9503.
18. Deddish, P. A., Wang, L. X., Jackman, H. L., Michel, B., Wang, J., Skidgel, R. A., and Erdos, E. G. (1996) *J. Pharmacol. Exp. Ther. 279*, 1582−1589.
19. Michaud, A., Williams, T. A., Chauvet, M. T., and Corvol, P. (1997) *Mol. Pharmacol. 51*, 1070−1076.
20. Dive, V., Cotton, J., Yiotakis, A., Michaud, A., Vassiliou, S., Jiracek, J., Vazeux, G., Chauvet, M. T., Cuniasse, P., and Corvol, P. (1999) *Proc. Natl. Acad. Sci. U.S.A. 96*, 4330−4335.
21. Junot, C., Gonzales, M. F., Ezan, E., Cotton, J., Vazeux, G., Michaud, A., Azizi, M., Vassiliou, S., Yiotakis, A., Corvol, P., and Dive, V. (2001) *J. Pharmacol. Exp. Ther. 297*, 606−611.
22. Rousseau, A., Michaud, A., Chauvet, M. T., Lenfant, M., and Corvol, P. (1995) *J. Biol. Chem. 270*, 3656−3661.
23. Azizi, M., Rousseau, A., Ezan, E., Guyene, T. T., Michelet, S., Grognet, J. M., Lenfant, M., Corvol, P., and Menard, J. (1996) *J. Clin. Invest. 97*, 839−844.
24. Murayama, N., Hayashi, M. A., Ohi, H., Ferreira, L. A., Hermann, V. V., Saito, H., Fujita, Y., Higuchi, S., Fernandes, B. L., Yamane, T., and de Camargo, A. C. (1997) *Proc. Natl. Acad. Sci. U.S.A. 94*, 1189−1193.
25. Eisenthal, R., and Cornish-Bowden, A. (1974) *Biochem. J. 139*, 715−720.
26. Cornish-Bowden, A., and Eisenthal, R. (1974) *Biochem. J. 139*, 721−730.
27. Cornish-Bowden, A., and Eisenthal, R. (1978) *Biochim. Biophys. Acta 523*, 268−272.
28. Cornish-Bowden, A., Porter, W. R., and Trager, W. F. (1978) *J. Theor. Biol. 74*, 163−175.
29. Holtz, B., Cuniasse, P., Boulay, A., Kannan, R., Mucha, A., Beau, F., Basset, P., and Dive, V. (1999) *Biochemistry 38*, 12174−12179.
30. Vazeux, G., Cotton, J., Cuniasse, P., and Dive, V. (2001) *Biochem. Pharmacol. 61*, 835−841.
31. Horovitz, A., and Levitzki, A. (1987) *Proc. Natl. Acad. Sci. U.S.A. 84*, 6654−6658.
32. Kuzmic, P. (1996) *Anal. Biochem. 237*, 260−273.
33. Araujo, M. C., Melo, R. I., Del Nery, E., Alves, M. F., Juliano, M. A., Casarini, D. E., Juliano, L., and Carmona, A. K. (1999) *J. Hypertens. 17*, 665−672.
34. Araujo, M. C., Melo, R. L., Cesari, M. H., Juliano, M. A., Juliano, L., and Carmona, A. K. (2000) *Biochemistry 39*, 8519−8525.
35. Ehlers, M. R., and Riordan, J. F. (1991) *Biochemistry 30*, 7118−7126.
36. Erdos, E. G., Deddish, P. A., and Marcic, B. M. (1999) *Trends Endocrinol. Metab. 10*, 223−229.
37. Marcic, B., Deddish, P. A., Jackman, H. L., and Erdos, E. G. (1999) *Hypertension 33*, 835−843.
38. Marcic, B., Deddish, P. A., Jackman, H. L., Erdos, E. G., and Tan, F. (2000) *Hypertension 36*, 116−121.

BI012121X